ties of the SIMPLE Pressure-Correction Algorithm," *International Journal for Numerical Methods in Fluids*, Vol. 8, 1988, pp. 441-461.
[6]Durst, F., Melling, A., and Whitelaw, J. H., "Low Reynolds Number Flow over a Plane Symmetric Sudden Expansion," *Journal of Fluid Mechanics*, Vol. 64, 1974, pp. 111-128.

Extension of the λ Formulation to Imperfect Gas Flows

Diego Lentini*
Università degli Studi di Roma "La Sapienza," I-00184 Rome, Italy

I. Introduction

A WIDE class of nozzle flows, including in particular those in air-breathing engines and wind tunnels (except the ones operating in the hypersonic range), involve large temperature excursions, but with stagnation values limited to 2000-2500 K. In such conditions, whereas chemical reactions can still be considered negligible, effects related to the specific heat varying with the temperature cannot. Indeed, specific heat at constant pressure c_p exhibits a fairly large variation with temperature. For example, the c_p of air varies by $\sim 25\%$ in the temperature range 200-2000 K (thermal equilibrium is assumed; see Sec. IV for a discussion of this assumption). At the same time, in the flows under consideration, the thermal equation of state is still closely obeyed. Such behavior must be taken into account in computational models if accurate numerical predictions are required.

The λ formulation[1,2] has proven to be a powerful tool for the numerical solution of compressible flows of a perfect gas. By "perfect" we mean that the gas is assumed to be both thermally and calorically perfect. The first attribute refers to its obeying the perfect gas law, and the latter denotes that its c_p is taken as a constant. This formulation has been successfully extended to finite-rate chemically reacting flows,[3-5] but with the limitation that the component gases of the reacting mixture are perfect.

In this Note we extend the λ formulation to (inert) flows of thermally perfect gas with c_p varying as a function of the temperature T. Such gases are sometimes referred to as "imperfect gases." The resulting formulation is extremely simple and involves a minimum computational overhead in comparison to the perfect gas case. Indeed, existing algorithms for a perfect gas can easily be upgraded with a minimum coding effort, without fundamentally altering their structure.

The proposed formulation is applied to the computation of flow in a quasi-one-dimensional nozzle to prove the workability of this approach and to demonstrate the differences with respect to a perfect gas computation. It will be apparent, however, that the range of application of the present formulation is completely general.

It should be noted that, at temperatures above the range considered here, reaction must inevitably be taken into account. However, this involves completely redefining both the model and the computational algorithm, with associated problems of an entirely different magnitude and much longer computer times. Further, the problem of caloric imperfection must still be addressed at the level of the individual component gases. Instead, the aim of the present paper is to show that within the stated assumptions a significantly better physical description can be achieved at a minimum cost with respect to a standard formulation.

Received May 10, 1991; revision received Feb. 18, 1992; accepted for publication March 7, 1992.

*Researcher, Dipartimento di Meccanica e Aeronautica. Member AIAA.

II. Formulation

The formulation is presented here for simplicity for a quasi-one-dimensional isentropic flow. We assume the speed of sound a as the state variable, and the velocity u as the motion variable. Consequently, the continuity and momentum equations, which we write for convenience in the form

$$a\frac{\rho_t + u\rho_x}{\rho} + au_x = -au\frac{A_x}{A} \tag{1}$$

$$u_t + uu_x + \frac{1}{\rho}p_x = 0 \tag{2}$$

will be recast in terms of the variables a and u. To this end, we observe that the speed of sound is related to the temperature T via the relationship

$$a^2 = \gamma RT \tag{3}$$

where γ is the gas specific heats ratio c_p/c_v, with $R = c_p - c_v$. After logarithmic differentiation we obtain

$$2\frac{a'}{a} = \left(1 + \frac{\gamma_T T}{\gamma}\right)\frac{T'}{T} \tag{4}$$

where the prime denotes differentiation with respect to either t or x, and γ_T is the derivative of γ with respect to T. From the first principle of thermodynamics, written for adiabatic flows with pressure work only,

$$c_v T' = RT\frac{\rho'}{\rho} \tag{5}$$

from which, in view of Eq. (4),

$$\frac{\rho'}{\rho} = \frac{1}{\delta\left(1 + \frac{\gamma_T T}{\gamma}\right)}\frac{a'}{a}$$

with the definition $\delta = (\gamma - 1)/2$. This expression will be substituted into the continuity equation.

The pressure gradient term in the momentum equation can be expressed by means of Gibbs' relationship, which in particular for isentropic flow reduces to

$$\frac{1}{\rho}p' = h'$$

where h is the enthalpy. Then, after Eq. (4), with $h' = c_p T'$,

$$\frac{1}{\rho}p_x = \frac{1}{\delta\left(1 + \frac{\gamma_T T}{\gamma}\right)}aa_x$$

The set of Eqs. (1) and (2) can then be recast as

$$\frac{1}{\delta\left(1 + \frac{\gamma_T T}{\gamma}\right)}(a_t + ua_x) + au_x = -au\frac{A_x}{A} \tag{6}$$

$$u_t + uu_x + \frac{1}{\delta\left(1 + \frac{\gamma_T T}{\gamma}\right)}aa_x = 0 \tag{7}$$

At this juncture, we note that the term a' can be expressed alternatively as $a_T T'$, with a being a function of the temperature T only. We also note that the term

$$\frac{1}{\delta\left(1 + \frac{\gamma_T T}{\gamma}\right)}a_T = \frac{1}{\gamma - 1}\sqrt{\frac{\gamma R}{T}} = \frac{c_p}{a}$$

is solely a function of the temperature only, as well. We can thus define the function

$$F(T) = \int_{T_0}^{T} \frac{c_p(\theta)}{a(\theta)}\, d\theta \tag{8}$$

where θ is the temperature as a running integration variable and T_0 is an arbitrary reference temperature. Notice that the integrand is always positive, so that the function $F(T)$ is monotonic and can easily be inverted. This definition allows the terms in the derivative of a in Eqs. (6) and (7) to be expressed as

$$\frac{1}{\delta\left(1 + \dfrac{\gamma_T T}{\gamma}\right)} a_t = F_t$$

and similarly for the derivative with respect to x. We can then recast Eqs. (6) and (7) in terms of the new variable F as

$$F_t + uF_x + au_x = \beta \tag{9}$$

$$u_t + uu_x + aF_x = 0 \tag{10}$$

with $\beta = -auA_x/A$. By summing and subtracting Eqs. (9) and (10), and defining

$$\lambda_1 = u + a, \qquad \lambda_2 = u - a$$

we obtain the final form:

$$R_{1t} + \lambda_1 R_{1x} = \beta \tag{11}$$

$$R_{2t} + \lambda_2 R_{2x} = \beta \tag{12}$$

having defined the Riemann variables as

$$R_1 = F + u, \qquad R_2 = F - u$$

Thus, the new variable F allows the Riemann variables for imperfect gas flows to be expressed as linear combinations, with constant coefficients, of the dependent quantities. This is analogous with the formulation for a perfect gas. For the case of strictly one-dimensional flow, such variables represent true Riemann invariants. Further, the imperfect gas formulation becomes formally identical to the perfect gas one. It is therefore apparent that the present formulation can be extended without difficulty to multidimensional flows, following the guidelines of previous work,[6] by redefining the Riemann variables in a similar fashion.

III. Solution Algorithm

As an example of the present formulation, we apply it here to the flow in a converging/diverging nozzle. We consider the steady-state solution only. A semi-implicit algorithm, developed along the guidelines of Moretti's fast solver,[7] is used. In this iterative technique Eqs. (11) and (12) are integrated separately, at each step, by successive sweeps over all of the computational domain.

The discretized form of Eq. (11) is, with second-order upwind differencing,

$$\frac{R_{1,n} - \hat{R}_{1,n}}{\Delta t} + \bar{\lambda}_1 \frac{R_{1,n} - R_{1,n-1}}{\Delta x} = \bar{\beta}$$

as λ_1 is always positive in the flow under consideration. The averages are defined as

$$\bar{\lambda}_1 = \frac{\lambda_{1,n} + \lambda_{1,n-1}}{2}, \qquad \bar{\beta} = \frac{\beta_n + \beta_{n-1}}{2}$$

The caret denotes the previous iteration level. Concerning Eq. (12), we have to make a distinction between the cases $\lambda_2 > 0$ and $\lambda_2 < 0$. In the former case (supersonic flow) the discretization is analogous to that for R_1:

$$\frac{R_{2,n} - \hat{R}_{2,n}}{\Delta t} + \bar{\lambda}_2 \frac{R_{2,n} - R_{2,n-1}}{\Delta x} = \bar{\beta}$$

with

$$\bar{\lambda}_2 = \frac{\lambda_{2,n} + \lambda_{2,n-1}}{2}, \qquad \bar{\beta} = \frac{\beta_n + \beta_{n-1}}{2}$$

whereas for $\lambda_2 < 0$ (subsonic flow) we get

$$\frac{R_{2,n} - \hat{R}_{2,n}}{\Delta t} + \bar{\lambda}_2 \frac{R_{2,n+1} - R_{2,n}}{\Delta x} = \bar{\beta}$$

with

$$\bar{\lambda}_2 = \frac{\lambda_{2,n} + \lambda_{2,n+1}}{2}, \qquad \bar{\beta} = \frac{\beta_n + \beta_{n+1}}{2}$$

Astride the sonic line the accuracy of the algorithm is reduced to first order by setting

$$\bar{\lambda}_1 = \lambda_{1,n}, \qquad \bar{\lambda}_2 = \lambda_{2,n}, \qquad \bar{\beta} = \beta_n$$

in order not to violate the domains of dependence of the variables. The equation in R_1 is integrated by sweeping in the positive x direction, whereas the one in R_2 is integrated by sweeping from the sonic line to the exit (supersonic region) and from the sonic line to the inlet (subsonic region). This algorithm gives a very fast convergence to the steady solution. For the case of imperfect gas, the procedure is initialized by first guessing the temperature field and then accordingly estimating F via the relationship

$$F = F(T) \tag{13}$$

as in Eq. (8). The a field is analogously initialized by means of the relationship

$$a = a(T) \tag{14}$$

as in Eq. (3). This allows λ_1 and λ_2 to be computed. Then at each iteration step the new values of R_1 and R_2 are computed, and u and F are updated as

$$u = \frac{R_1 - R_2}{2}, \qquad F = \frac{R_1 + R_2}{2}$$

The speed of sound is then recomputed as

$$a = a(F) \tag{15}$$

where the argument of Eq. (14) has been transformed into F by inverting Eq. (13). The propagation speeds λ_1 and λ_2 can then be recomputed and a new iteration cycle can be started, until convergence is attained.

The boundary condition at the inlet involves matching the total enthalpy:

$$h_0 = h + (u^2/2)$$

where h is recovered as

$$h = h(F) \tag{16a}$$

with the stagnation enthalpy h_c, i.e.,

$$h_c = h(R_2 + u) + (u^2/2) \tag{16b}$$

where F is expressed via the value of R_2 as determined by the left-sweeping integration procedure in the subsonic region.

Equation (16b) is nonlinear in u and is solved by iteration to determine the value thereof at the inlet. Once the converged solution is obtained, the density can be recovered as a function of F, via Eq. (5):

$$\log \frac{\rho}{\rho_0} = \frac{1}{R} \int_{T_0}^{T} \frac{c_v(\theta)}{\theta} \, d\theta \tag{17}$$

The pressure is then computed by means of the (thermal) equation of state.

In the present implementation the functions defined by Eqs. (13–17) are computed off-line and approximated by fourth-order fits, obtained by means of orthogonal polynomials, to make the computational procedure as straightforward as possible.

IV. Results and Discussion

We show here a comparison between a calculation performed for a perfect gas (with $\gamma = 1.4$) and the present approach for an imperfect gas, by considering critical flow in a converging/diverging nozzle. The working fluid is assumed to be air, with caloric properties modeled as a function of the temperature by means of the so-called NASA polynomials (e.g., see Ref. 8). A nozzle with conical converging (semiangle 45 deg) and diverging (semiangle 15 deg) sections, matched by a throat section with a circular profile, is considered. The inlet and throat radii are in the ratio 0.19 to 0.12 (note that in the present formulation results are independent of the scale of length, as in perfect gas flows); the radius of curvature of the throat is equal to the throat radius, and the geometric expansion ratio (exit to throat area) is 5. The stagnation temperature T_c is assumed to be 2000 K (note that for imperfect gases results do not scale with temperature). Although at this high temperature some molecular dissociation and formation of nitric oxides do occur, a chemical equilibrium computation (performed with the code by Reynolds[9]) shows that the cumulative mass fraction of the ensuing products is $<1\%$, except for pressures below 0.002 atm; incidentally, finite-rate chemistry effects lead to nitric oxide concentrations well below the equilibrium values in most situations. Accordingly, in this study we neglect effects related to varying composition. In particular, the variation in the average molecular weight turns out to be absolutely negligible. A computational grid with 40 nodes is chosen; for a perfect gas it yields a relative discrepancy between the analytical and numerical solutions limited to 0.7% (in terms of Mach number).

Figure 1 compares axial profiles of velocity u for the two cases of a perfect and an imperfect gas, with the same stagnation conditions. The nozzle profile is superimposed on the figure. In the same fashion Fig. 2 compares axial profiles of Mach number, and Fig. 3 compares profiles of temperature. It can be observed that, although u and M are affected to a limited extent by the varying c_p, the temperature computed with the imperfect gas model exhibits a sensibly slower decay than the perfect gas solution because of the higher specific heat. In particular, the gap between the two solutions at the outlet exceeds 150 K, thus underlining the need to account correctly for the caloric properties of the gas. Further, neglecting the effects of temperature on c_p leads to overestimating the mass flow rate by 4.1% and the velocity thrust by 1.5%; accordingly, the specific impulse is underestimated by 2.5%. Notice that for air-breathing engines a consistently larger effect is produced on the *net* thrust and specific impulse.

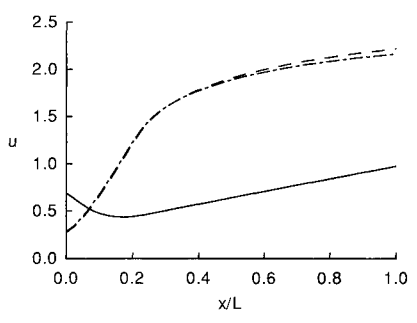

Fig. 1 Axial profiles of velocity u (made dimensionless with the reference value $\sqrt{RT_c}$). Dashed-dotted line, perfect gas; dashed line, imperfect gas; solid line, nozzle contour.

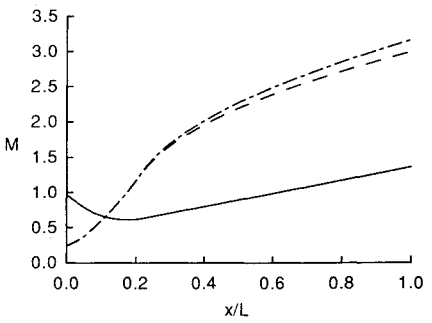

Fig. 2 Axial profiles of Mach number M. Dashed-dotted line, perfect gas; dashed line, imperfect gas; solid line, nozzle contour.

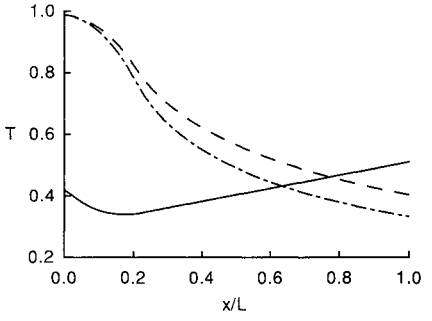

Fig. 3 Axial profiles of temperature T (made dimensionless with the reference value T_c). Dashed-dotted line, perfect gas; dashed line, imperfect gas; solid line, nozzle contour.

The present model assumes that the gas is in thermal equilibrium, i.e., that the characteristic time for vibrational relaxation τ_v is small compared to the characteristic local flow time τ_f. This can be quantified by a vibrational Damköhler number, defined as

$$Da_v = \frac{\tau_f}{\tau_v}$$

which must then be much larger than one for the present model to hold. This condition is checked for the test case under consideration as follows. A local flow time is introduced as the inverse of the rate of change of the vibrational energy e_v brought about by the gasdynamic expansion[10]

$$\tau_f = -\left[\frac{u}{e_v}\frac{de_v}{dx}\right]^{-1}_{eq}$$

where the subscript eq indicates that the term is computed assuming vibrational equilibrium (entailing that e_v is a function of the temperature). For τ_v we adopt the approximate form of the Landau and Teller model[11]:

$$\tau_v = (C_1/p)\exp(C_2/T)^{1/3}$$

and refer to the slowest vibrational relaxation process (which for the present case is de-excitation of N_2 by collision with other N_2 molecules). Notice that, unlike equilibrium quantities, Da_v depends on the scale of length (taken here as the length L_d of the nozzle divergent section) and the pressure level (identified by the stagnation pressure p_c), besides the temperature scale. Figure 4 reports the axial profiles of Da_v, with $p_c L_d$ as a parameter. It is seen that the assumption of

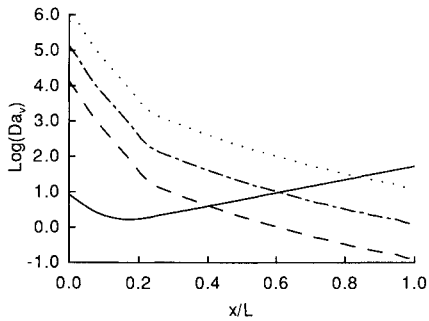

Fig. 4 Axial profiles of vibrational Damköhler number Da_v. Dashed line, p_cL_d = 10 kPa-m; dashed-dotted line, p_cL_d = 100 kPa-m; dotted line, p_cL_d = 1000 kPa-m; solid line, nozzle contour.

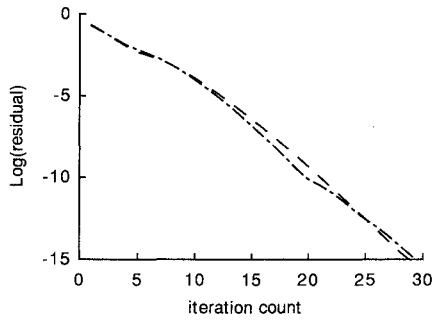

Fig. 5 Decay of the residual of the computation. Dashed-dotted line, perfect gas; dashed line, imperfect gas.

thermal equilibrium is satisfied in most parts of the nozzle but fails in the final part of the divergent section for low values of p_cL_d (i.e., for short nozzles operating at a low stagnation pressure). For $Da_v \ll 1$ the gas behavior is better represented by assuming c_p to be constant. In applications to high-expansion-ratio nozzles a "sudden freezing" model[10,12] can be used to bridge regions computed under the hypotheses of thermal equilibrium (i.e., imperfect gas) and vibrationally frozen flow (perfect gas). The results shown in Fig. 4 are conservative in that the actual rates of vibrational relaxation are faster than assumed here. In typical shock tunnel flows the vibrational relaxation rates are known to be faster than those given by the Landau-Teller model by a factor between 3 and 100 (Ref. 13). When this phenomenon is accounted for, the range of applicability of the present work becomes much wider than that shown in the figure.

Figure 5 compares the convergence history of the computations for a perfect and an imperfect gas. The solution is initialized by prescribing the same (arbitrary) Mach number distribution in both cases. It is apparent that the solution algorithm described in Sec. III gives an extremely fast convergence rate, with the steady state reached in as few as 30 iterations.

V. Conclusions

The proposed formulation demonstrates the possibility of effectively extending all computational techniques developed for the λ formulation to imperfect gas flows, with minimum coding and computational effort.

References

[1]Moretti, G., "The λ-Scheme," *Computers & Fluids,* Vol. 7, No. 3, 1979, pp. 191–205.

[2]Moretti, G., "An Efficient Euler Solver, with Many Applications," AIAA Paper 87-0352, Jan. 1987.

[3]Lentini, D., and Onofri, M., "Solutore Numerico Veloce per Flussi Chimicamente Reagenti in Nonequilibrio," *L'Aerotecnica Missili e Spazio,* Vol. 65, No. 3, Sept. 1986, pp. 110–118.

[4]Lentini, D., and Onofri M., "Nonequilibrium Chemically Reacting Flows in Nozzles," *Analysis and Design of Advanced Energy Systems: Fundamentals,* Vol. 3-1, edited by M. J. Moran and R. A. Gaggioli, American Society of Mechanical Engineers, AES, New York, 1987, pp. 33–40.

[5]Lentini, D., and Onofri, M., "Fast Numerical Technique for Nozzle Flows with Finite-Rate Chemical Kinetics," *Computational Fluid Dynamics,* Proceedings II International Symposium on Computational Fluid Dynamics, North-Holland, Amsterdam, 1988, pp. 449–460.

[6]Moretti, G., and Zannetti, L., "A New, Improved Computational Technique for Two-Dimensional Unsteady Compressible Flows," AIAA Paper 82-0168, Jan. 1982.

[7]Moretti, G., "A Fast Euler Solver for One-Dimensional Flows," NASA CR 3689, June 1983.

[8]"Table of Coefficient Sets for NASA Polynomials," *Combustion Chemistry,* edited by W. C. Gardiner, Springer-Verlag, New York, 1984, pp. 485–504.

[9]Reynolds, W. C., "The Element Potential Method for Chemical Equilibrium Analysis: Implementation in the Interactive Program STANJAN," Dept. of Mechanical Engineering, Stanford Univ., Stanford, CA, Jan. 1986.

[10]Bray, K. N. C., "Chemical and Vibrational Nonequilibrium in Nozzle Flows," *Nonequilibrium Flows,* Vol. 1, Part II, edited by P. P. Wegener, Dekker, New York, 1970, pp. 70–75, 93–98.

[11]Vincenti, W. G., and Kruger, C. H., *Introduction to Physical Gas Dynamics,* Wiley, New York, 1965, pp. 198–206.

[12]Phinney, R., "Criterion for Vibrational Freezing in a Nozzle Expansion," *AIAA Journal,* Vol. 1, No. 2, 1963, pp. 496–497.

[13]Hurle, I. R., "Nonequilibrium Flows with Special Reference to the Nozzle-Flow Problem," *Proceedings of the 8th International Shock Tube Symposium,* Chapman and Hall, London, 1971, pp. 3/1–3/37.

Surface Reaction Model for Catalyzed Composite Solid Propellants

S. Krishnan* and R. Jeenu†
Indian Institute of Technology, Madras 60036, India

Nomenclature

A = kinetic pre-exponential factor
A_{fc} = oxidizer particle area fraction of the enhanced condensed phase exothermic decomposition
c_p = average specific heat capacity for the solid and gases
D_0 = oxidizer particle diameter
E = activation energy
K = constant dependent on type of catalyst and surface/subsurface reaction
m = mass flux
Q = heat release
R = universal gas constant
S = surface area
T = temperature
α = mass fraction of ingredient in propellant
β_F = fraction of oxidizer that partake in primary flame reaction
Γ = catalyst specific surface dependent constant
ϵ = ratio of oxidizer decomposed due to a condensed phase exothermic decomposition to the total oxidizer decomposed
λ = thermal conductivity
Φ = stoichiometric oxidizer/fuel ratio
ρ = density
ξ^* = dimensionless flame height

Received March 9, 1991; revision received Jan. 2, 1992; accepted for publication Jan. 22, 1992.

*Professor, Department of Aerospace Engineering. Senior Member AIAA.

†Research Associate, Department of Aerospace Engineering.